

Supplementary Materials for
A cellular resolution atlas of Broca's area

Irene Costantini *et al.*

Corresponding author: Irene Costantini, costantini@lens.unifi.it

Sci. Adv. **9**, eadg3844 (2023)
DOI: 10.1126/sciadv.adg3844

The PDF file includes:

Figs. S1 to S4
Legends for movies S1 to S4

Other Supplementary Material for this manuscript includes the following:

Movies S1 to S4

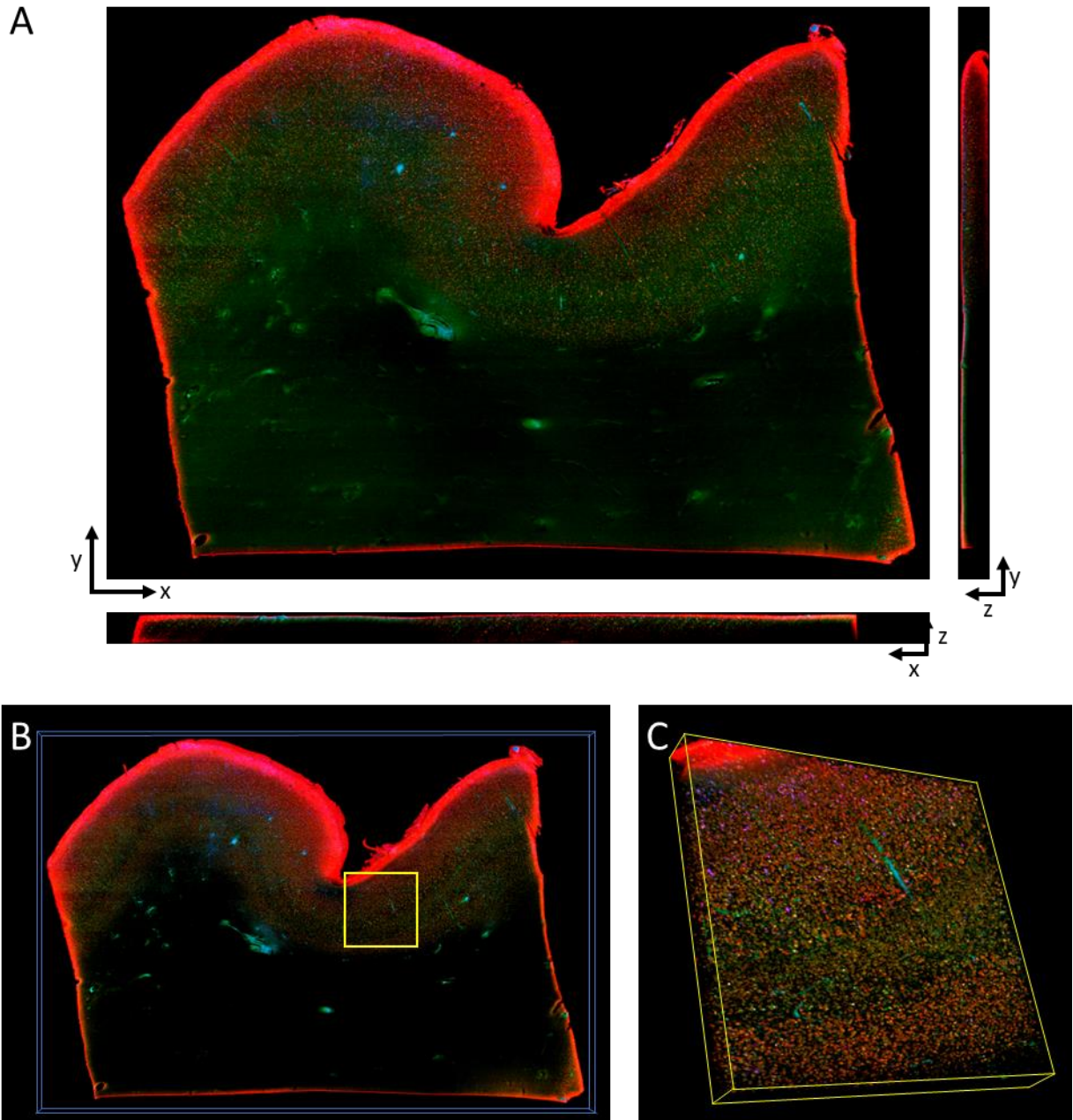


Fig. S1. LSFM 3D reconstruction. (A) Orthogonal views of a representative slice immunostained for CR (calretinin) in blue, PI (propidium iodide) in green, and NeuN in red (the xy plane displays the reconstruction at $\sim 180 \mu\text{m}$ depth). (B) 3D rendering of the slice in A ($1500 \times 1300 \times 0.5 \text{ mm}^3$). (C) 3D rendering of the yellow box in B ($2 \times 2 \times 0.5 \text{ mm}^3$). (B) and (C) images were produced using the plugin “3D Viewer” of Fiji.

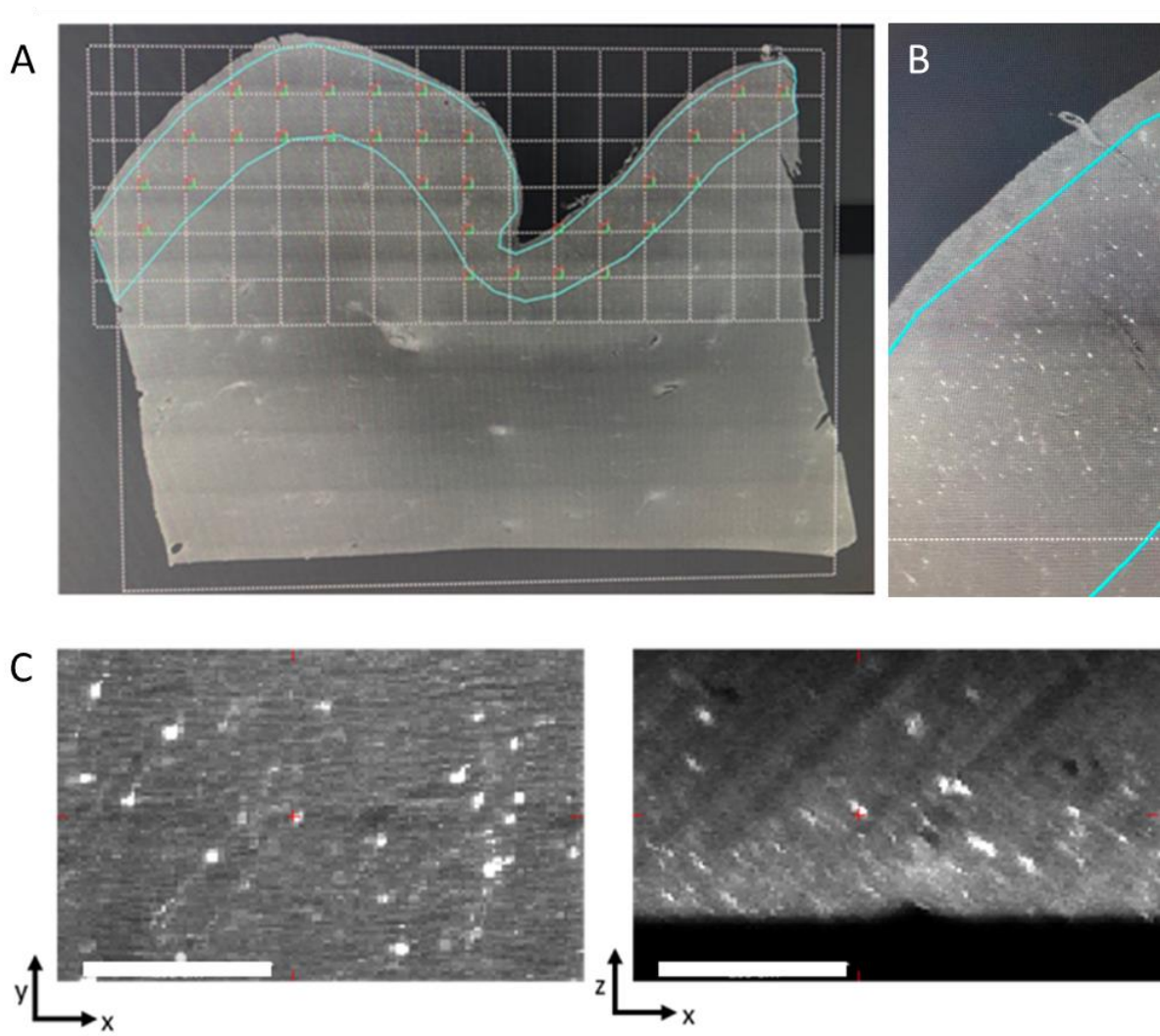


Fig. S2. Stereologic quantification of CR+ interneurons from LSFM images. (A) A slab immunostained for CR from the LSFM imaging dataset displaying a systematic-random counting grid employed during stereologic analyses. (B) Zoomed-in image displaying cortical layer 3. (C) Insets showing the native resolution (3.3 μm isotropic) along the three axes. Grid size on (A) = 800 μm, scale bars on (C) = 200 μm.

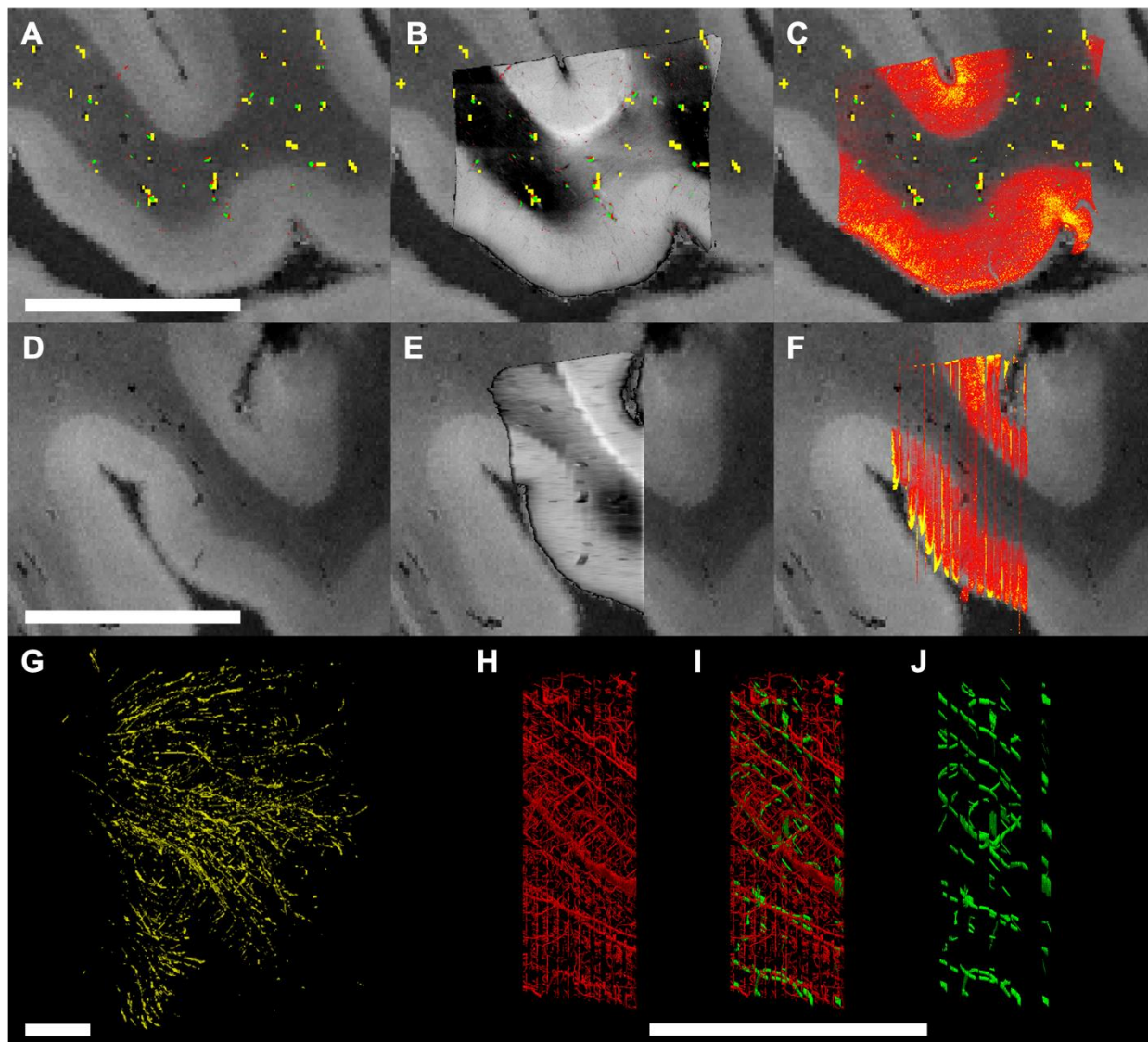


Fig. S3. Vasculature segmentation and alignment. Vessels with a radius larger than $150\ \mu\text{m}$ were manually segmented in the MRI volume (**A**) and in each LSFM slice (**C**). A semi-automated method based on the Frangi filter was used to segment vessel-like structures in the PSOCT volume (**B**). The second row shows aligned and reconstructed volumes of MRI (**D**), OCT (**E**) and LSFM (**F**) across the slice direction. Segmented vessels in each modality are also shown in 3D (**G**: MRI, **H**: OCT, **J**: LSFM). Panel (**I**) displays LSFM vessels (in green) across all

slices after reconstruction by non-linear coregistration with the PSOCT volume, overlaid with PSOCT vessels (in red). Scale bars = 1 cm.

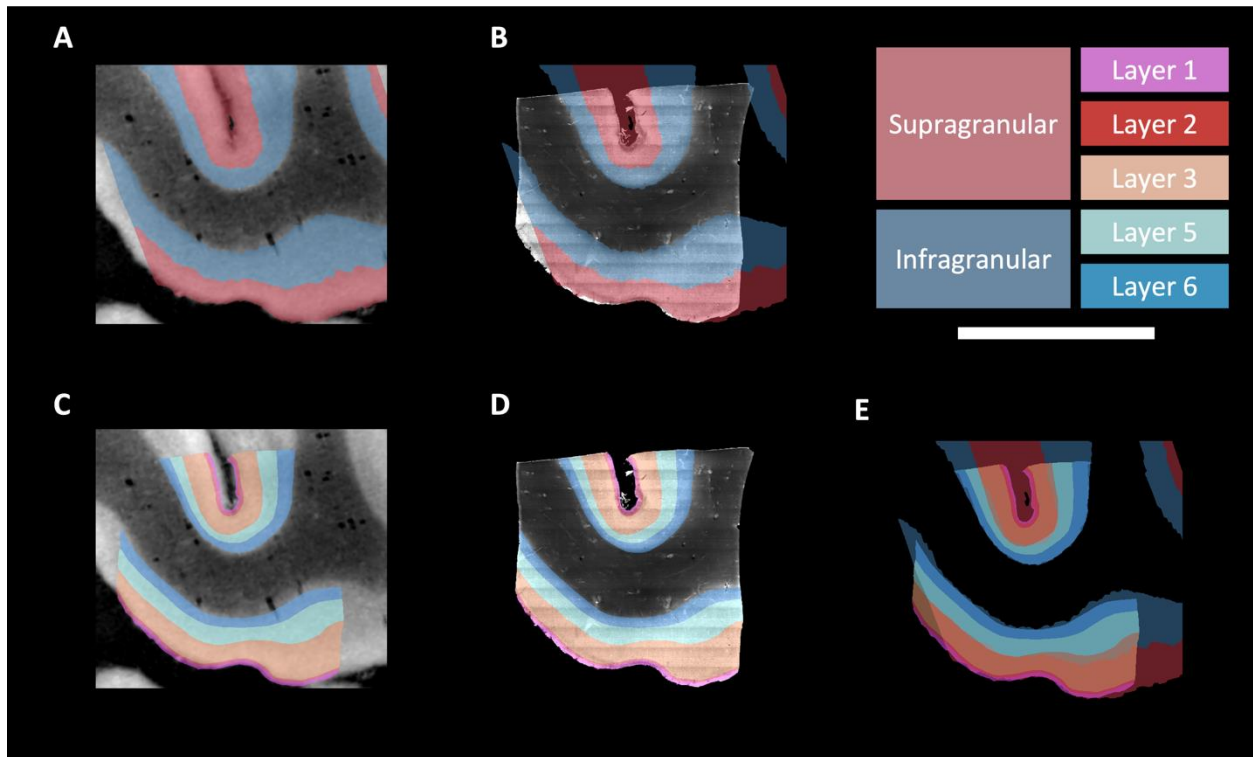


Fig. S4. Visual assessment of the alignment of infragranular and supragranular layers across MRI and LSFM, after coregistration. Infragranular and supragranular labels derived from MRI (A) are overlaid with LSFM in (B). Similarly, laminar labels derived from LSFM (D) are overlaid with MRI in (C). Finally, both labels are overlaid in (E). Scale bar = 1cm.

Movie S1.

3D rendering of the 16 slices acquired with OCT for a total volume of $1.5 \times 1.3 \times 0.8 \text{ cm}^3$

Movie S2.

Navigation in the 3D rendering of a representative slice acquired with LSFM and stained with anti-CR antibody in blue ($\lambda_{exc} = 488$), Propidium Iodide (nuclei) in green ($\lambda_{exc} = 561$), and anti-NeuN antibody in red ($\lambda_{exc} = 638$).

Movie S3.

Navigation across sagittal MRI slices and zoom into Broca's area. Coregistered slices of OCT, LSFM (stained for PI, CR and NeuN) and manually segmented cortical layers are displayed in the same space.

Movie S4.

Navigation across sagittal MRI slices in Broca's area, with coregistered stereological counts of NeuN+ neurons (green) and CR+ neurons (red) overlaid.